Nuclear Physics B285 [FS19] (1987) 590–605
North-Holland, Amsterdam

# PHOTON AND BOSONIUM MASSES IN SCALAR LATTICE QED*

H.G. EVERTZ[1], K. JANSEN[1], J. JERSÁK[1], C.B. LANG[2] and T. NEUHAUS[3]

[1] *Institut für Theoretische Physik E, RWTH Aachen, D-5100 Aachen, W. Germany*
[2] *Institut für Theoretische Physik, Universität Graz, A-8010 Graz, Austria*
[3] *Supercomputer Computations Research Institute, FSU, Tallahassee, FL 32306, USA*

Received 12 February 1987

We analyze the particle spectrum of the compact U(1) lattice gauge theory with a scalar matter field of unit charge. The nonperturbative Monte Carlo calculation is performed on lattices of sizes $8^3 \times 16$, $12^4$ and $16^4$. In the Coulomb phase we find a massless photon and massive scalar and vector bosonium states which are neutral bound states of charged bosonic particles, analogous to the positronium in QED. In the Higgs region of the confinement-Higgs phase the massive photon and the Higgs boson are present. Here we do not find any other vector state with a mass substantially different from the photon mass.

## 1. Introduction

The main incentive for a systematical study of Higgs models (coupled gauge and scalar fields) on the lattice is to improve our understanding of the standard model of electroweak interactions from the nonperturbative point of view. Of particular interest is the Higgs mechanism for the mass generation of vector bosons. According to the present knowledge, this mechanism may be understood without including the fermionic matter fields.

The formulation of Higgs models on an euclidean space-time lattice is straightforward [1, 2] and the numerical approach well understood [3]. In contrast to gauge theories with fermion matter fields, the Higgs models have always been implemented as a complete coupled system of compact gauge link variables and scalar site variables. At the beginning, the discussion was restricted to the abelian fixed length scalar fields [4]. (For an extensive list of references on lattice Higgs models see the review article, ref. [5].) Soon it was realized that inclusion of the dynamics of the radial mode opens the view on a more structured phase landscape [6, 7, 5], in particular in the case of the compact U(1) model [8, 9], and many later studies of the Higgs models have taken the radial mode into account.

* Work supported by the project P5965 of "Fonds zur Förderung der Wissenschaftlichen Forschung in Österreich", the Deutsches Bundesministerium für Forschung und Technologie and the Deutsche Forschungsgemeinschaft.

The full gauge symmetry group of the electroweak theory is SU(2) × U(1) and some recent studies [10] have been concerned with the corresponding Higgs model. The simplest lagrangian of this model involves, however, already four coupling constants. For that reason we decided to investigate first the basic properties of the system separately for the nonabelian gauge group SU(2) [7,11,12] and for the abelian group U(1) [9]. The latter Higgs model, which may also be looked upon as scalar QED, will be discussed here. In recent presentations [9] we concentrated on the precise determination of the phase structure and on a study of the nature of the phase transitions. Here we want to present our Monte Carlo results on the mass spectrum of the U(1) Higgs model with a scalar field of unit charge. In another paper [13] we present the results for the Wilson loops and gauge invariant two-point functions obtained in the same Monte Carlo runs.

For completeness we briefly review the notation [7,9]. The action on the four-dimensional euclidean lattice may be cast in the three-parameter form

$$S = -\tfrac{1}{2}\beta\sum_{\mathrm{p}}\left(U_{\mathrm{p}} + U_{\mathrm{p}}^*\right) - \kappa\sum_x\sum_\mu\left(\Phi_x^* U_{x,\mu}\Phi_{x+\mu} + \mathrm{c.c.}\right)$$
$$+\lambda\sum_x\left(\Phi_x^*\Phi_x - 1\right)^2 + \sum_x \Phi_x^*\Phi_x . \tag{1.1}$$

The plaquette variables $U_{\mathrm{p}}$ denote the product of link fields $U_{x,\mu}$ around the plaquettes. The action exhibits various invariances (like e.g. $\kappa \leftrightarrow -\kappa$) which are discussed in refs. [7,9] together with the relationship to the corresponding action in the continuum.

The link, plaquette and scalar field variables are complex numbers but may be represented by real variables,

$$U_{x,\mu} = \exp\left(i\varphi_{x,\mu}\right), \qquad U_{\mathrm{p}} = \exp\left(i\varphi_{\mathrm{p}}\right), \qquad \Phi_x = \rho_x \exp\left(i\varphi_x\right). \tag{1.2}$$

In these variables, which we use for numerical simulation, the action assumes the form

$$S = -\beta\sum_{\mathrm{p}}\cos\varphi_{\mathrm{p}} - 2\kappa\sum_x\sum_\mu \rho_x\rho_{x+\mu}\cos\left(\varphi_{x+\mu} - \varphi_x + \varphi_{x,\mu}\right)$$
$$+\lambda\sum_x\left(\rho_x^2 - 1\right)^2 + \sum_x \rho_x^2 . \tag{1.3}$$

The action (1.3) defines the Boltzmann factor that determines the probability distribution of the field configurations. For given couplings an ensemble of configurations is generated by standard Monte Carlo techniques. In our calculations the gauge group U(1) was approximated by the discrete subgroup Z(60) for practical reasons. Possible caveats of this approximation have been discussed in earlier work [9], where also some details of our program have been described.

Let us briefly recall the essentials of the phase structure. At $\kappa = 0$ the model reduces to the pure U(1) compact gauge model. For $\beta = \infty$ the system describes the two-component $\Phi^4$ theory. In the limit $\lambda \to \infty$ the radial mode of the Higgs doublet freezes and $|\Phi_x| = 1$. This is the case of the fixed length model. In ref. [9] the phase diagram was studied for various values of $\lambda$ between 0.001 and 10. There are two phases which are completely separated in the space of all coupling constants: the Coulomb phase and the confinement-Higgs phase.

The Coulomb phase is the analytic continuation of the corresponding phase for pure U(1) gauge theory to positive values of $\kappa$ and one expects to find the massless photon throughout this phase [1]. In this phase there should also exist a charged bosonic particle [13,14]. Pairs of these charged particles can form neutral bound states which we call bosonium in analogy to positronium in QED or quarkonium in QCD.

Increasing $\kappa$ (for constant $\lambda$ and $\beta$), one passes from the Coulomb phase through the so-called Higgs phase transition (PT) at $\kappa = \kappa_{\mathrm{PT}}$ to the Higgs region of the confinement-Higgs phase. This region is adjacent to the phase of broken global symmetry in the pure $\Phi^4$ theory at $\beta = \infty$. The most prominent property of the Higgs region is the linear dependence of the gauge invariant expectation value of the scalar field on $\kappa$ for sufficiently large $\kappa > \kappa_{\mathrm{PT}}$ [8,9]:

$$\langle \Phi^* \Phi \rangle \simeq \frac{4}{\lambda} \kappa + \text{const}. \tag{1.4}$$

This indicates the presence of the scalar field condensate, in analogy to the quasiclassical picture of spontaneous symmetry breakdown. The Higgs region is analytically connected to the confinement region [1,2,15] which is adjacent to the confinement phase of the pure compact U(1) gauge model at $\beta < \beta_{\mathrm{PT}} \simeq 1$. In the confinement region, as also in the Coulomb phase, the values of $\langle \Phi^* \Phi \rangle$ are small and only weakly $\kappa$-dependent [8,9].

In the whole confinement-Higgs phase one expects, on the basis of the quasiclassical perturbative approach, the presence of the Higgs boson and of the massive photon. However, a richer, genuinely nonperturbative spectrum might be possible. The Higgs PT line extends into the confinement-Higgs phase where for $\lambda \geqslant O(1)$ it has an endpoint at some $\beta > 0$ and is rather weak [8,9]. For $\lambda \leqslant O(0.1)$ the line separates the confinement and the Higgs regions and clearly is of first order [8,9]. This change is related to the activation of the radial mode $\rho_x$ at small $\lambda$ [6]. Nevertheless, the confinement and Higgs regions are still analytically connected in the three-dimensional parameter space.

The Higgs PT between the Coulomb phase and the Higgs region is of first order for small $\lambda$ but becomes weaker for increasing $\lambda$ and $\beta$. For $\lambda = 3$ one can hardly decide the order of the phase transition. Recent results for the exponential decay of the gauge invariant two-point function of the scalar field gave indications that for this $\lambda$ and $\beta = 2.5$ the Higgs PT still is of a very weak first order [13].

For our study of the spectrum in the Coulomb phase and in the Higgs region we chose the values $\beta = 2.5$ and $\lambda = 3.0$ and varied only the bare Higgs coupling parameter $\kappa$. The Higgs PT on an $8^3 \cdot 16$ lattice then lies at $\kappa_{PT} = 0.179(1)$ and on $16^4$ at $\kappa_{PT} = 0.177(2)$. This choice of couplings was motivated from our earlier investigation of the phase diagram [9] which indicated the possibility of a second order Higgs PT for these values of $\beta$ and $\lambda$.

In sect. 2 we present our results for the masses of the states observed in both phases. In sect. 3 we summarize our results for the specific heat. We also describe the influence of metastable Dirac sheets [16] on various observables.

## 2. Determination of the masses

### 2.1. OPERATORS AND MEASUREMENTS

Let us begin with an introduction to the method and the technical details for calculation of the masses in the U(1)-Higgs model. We introduce the operators:

$$O_1(\boldsymbol{x}, t) = \mathrm{Re} \sum_{\mu} \Phi_x^* U_{x,\mu} \Phi_{x+\mu}, \tag{2.1}$$

$$O_2(\boldsymbol{x}, t) = \mathrm{Im} \sum_{\mu} \Phi_x^* U_{x,\mu} \Phi_{x+\mu}, \tag{2.2}$$

$$\mathrm{O}_3(\boldsymbol{x}, t) = \mathrm{Im} \sum_{\mu,\nu} U_{\mathrm{p}}, \tag{2.3}$$

$$x = (\boldsymbol{x}, t); \qquad \mathrm{p} = x\mu\nu; \qquad \mu, \nu = 1,2,3.$$

These lattice operators, summed over $\boldsymbol{x}$, as associated with quantum numbers $J^{PC} = 0^{++}$, $1^{--}$ and $1^{+-}$, respectively. (For procedures to construct operators with given quantum numbers see ref. [17].) To give these operators a 3-momentum in the 1-direction, we introduce

$$O_i(k, t) = \sum_{\boldsymbol{x}} O_i(\boldsymbol{x}, t) \exp(ik \cdot x_1), \tag{2.4}$$

where $k = p \cdot 2\pi/L$, and $L$ is the spatial size of the lattice. We considered only the values $p = 0$ and 1. The plaquette operator $O_3$ with momentum $p = 1$ is appropriate for a search for the expected massless photon state. It was pointed out in ref. [18] that in spite of the wrong parity of $O_3$ at $k = 0$ in comparison with the continuum photon, the corresponding correlation function with $k > 0$ gets contributions from the odd superposition of photon states with the same momentum and opposite helicities.

With these operators we calculated correlation functions

$$C_i(\Delta t) = \sum_t \langle (O_i(t) - \langle O_i(t) \rangle)(O_i(t+\Delta t) - \langle O_i(t+\Delta t) \rangle) \rangle , \tag{2.5}$$

where the sum goes over the time direction of the lattice. In order to estimate the statistical errors we blocked the results of the correlation measurements in blocks of 1000–1500 sweeps. The average of these block correlation functions over all blocks leads to final values and statistical errors. The correlation functions are then fitted according to

$$C_i(\Delta t) = \text{const}(e^{-E_i \Delta t} + e^{-E_i(L_t - \Delta t)}) , \tag{2.6}$$

where $L_t$ is the size of the periodic lattice in the time-like direction. For the fit of the data according to eq. (2.6) we discarded the points with $\Delta t = 0$ and 1. The masses $m_i$ are determined from the energies $E_i$ by means of the lattice dispersion relation. Both quantities are in lattice units.

Our results have been obtained on lattices of sizes $8^3 \times 16$, $12^4$, and $16^4$, with typically 150 000 iterations on the $8^3 \times 16$ lattice and 40 000 iterations on the other lattices. This wide variation of the lattice size allowed us to control the influence of the finite lattice size on our results. We used about 350 hours of Cyber-205 time for this and a parallel paper [13].

Most of our results are obtain in the vicinity of the Higgs PT. Further $\kappa$-points, where we performed calculations, are at $\kappa = 0$ and $\kappa = 0.1$ deep in the Coulomb phase, and $\kappa = 0.3$ and 0.64 in the Higgs region. The latter two points are distant enough from the Higgs PT to find the increase of the photon mass with $\kappa$.

### 2.2. RESULTS

In fig. 1 we exhibit our data for the photon propagator at momentum $p = 1$, for $\kappa = 0.1757 < \kappa_{PT}$. The solid line represents the correlation function in the case of a massless photon. The actual fit by means of the expression (2.6) is almost indistinguishable from this line and the value of $m_\gamma$ obtained in this fit is consistent with zero. For other $\kappa$-values the fits are of similar quality. The fits for the other correlation functions are also of good quality, as long as the energies are not larger than about 1. From these fits we find the following picture for the mass spectrum, shown in figs. 2 and 3:

*2.2.1. Coulomb phase.* Here we have observed three states. The lightest of them, the photon, has a mass consistent with zero. For the Coulomb phase in the pure U(1) compact lattice QED the existence of a massless state has been proven rigorously [19] and confirmed by Monte Carlo calculations both directly [18] and by establishing the coulombic form of the potential [20]. To our knowledge there is no rigorous result on the mass of the photon inside this free charge phase of the compact U(1) Higgs model (in contrast to the noncompact one [21]), but the photon

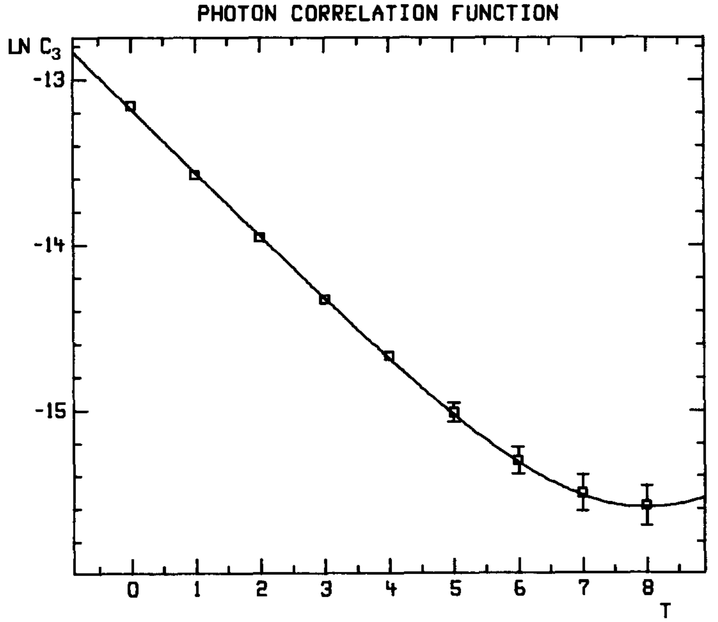


Fig. 1. Logarithm of the correlation function of operator $O_3$ at $p=1$, for $\kappa=0.1757$ on a $16^4$ lattice. The solid line represents the correlation function (2.6) for an energy of 0.388, corresponding to zero photon mass (eq. (2.12)). All data in figs. 1–4 are taken at $\lambda=3$, $\beta=2.5$.

is generally expected to be massless there, too [1]. A massless photon inside a phase with charged dynamical matter has also been found in Monte Carlo simulations of the SU(2) Higgs model with triplett matter field [22].

In our analysis we find, in the Coulomb phase, the massless photon through the $p=1$ correlation function of the operator $O_3$, but no signal at $p=0$. On the other hand the $p=1$ signal is very clear. The existence of the massless photon in the Coulomb phase is also supported by the coulombic form of the static potential determined by means of Wilson loops [13].

The other correlation functions decay very rapidly in the Coulomb phase except very close to the Higgs PT. Therefore states other than the photon appear to be very heavy with a mass larger than two inverse lattice units. In the vicinity of the Higgs PT, however, two massive states can be resolved. One of them has the same quantum numbers $0^{++}$ as the Higgs boson. Its mass decreases rapidly towards the phase transition down to a value of about 0.2 in inverse lattice units. The other state observed is a $1^{--}$ vector boson. It dominates the correlation function of the operator $O_2$ both for $p=0$ and $p=1$. We have found no measurable contribution of a massless state in this correlation function for $\kappa \leqslant 0.1765$. Of course, when the mass of the $1^{--}$ state drops to values of about 0.1–0.2, a contribution of the photon cannot be excluded.

We want to call these two heavy states in the Coulomb phase the scalar and vector *bosonium*. Our motivation for this name is the following: In the Coulomb phase the scalar lattice QED has an unconfined charged bosonic particle associated with the charged field $\Phi$. Neutral pairs of these particles interact both through the attractive coulombic force and the $\Phi^4$ coupling. It is not a priori clear whether they form bound states, but if they do so, these states should show up in the correlation functions of the operators containing $\Phi^*$ and $\Phi$ like (2.1) and (2.2). The mass $m_c$ of the unconfined charged particle may be estimated [13] from the data for the gauge invariant two-point function

$$G(x, y) = \left\langle \Phi_x^* \prod_{\ell \in \Gamma} U_\ell \Phi_y \right\rangle, \tag{2.7}$$

where $\Gamma$ is a path connecting the points $x$ and $y$. This function is related to the bound state of the charged particle with an external charge [13,14]. We find that the masses of both the scalar and vector bosonium are, at least for $0.175 \leqslant \kappa < \kappa_{PT}$, smaller than $2m_c$, at the same values of $\beta$ and $\lambda$. Thus their interpretation as a bound state of two bosonic charged particles is plausible.

Since the interaction of the charged particles via the quartic self-coupling is strong for our values of $\lambda$, there is no simple way to estimate the masses of the bosonium states on the basis of the known values of $m_c$. Actually the bosonium masses are much smaller than $2m_c$, indicating that the binding energy is large.

In order to provide some idea about the bare mass of these strongly interacting constituent particles, we determined the "current mass" $m_0$ from the relation to the distance from $\kappa_{PT}$, like for the free boson theory ($\beta = \infty$, $\lambda = 0$),

$$\frac{1}{\kappa} - \frac{1}{\kappa_{PT}} = 2(\cosh m_0 - 1). \tag{2.8}$$

This approach is essentially like the determination of the bare unquenched mass in the lattice QCD calculation for Wilson fermions [23]. The resulting mass $m_0$ is not renormalization invariant and gives only a rough idea on the magnitude of the screened constituent scalar field mass. In the range considered ($0.174 \leqslant \kappa \leqslant \kappa_{PT}$), the resulting values of $2m_0$ agree approximately with the scalar bosonium mass.

*2.2.2. Higgs region.* At the Higgs PT the photon mass shows, within our resolution, no discontinuity, and is compatible with zero even close above the PT. This agrees with the observation [13] that the static potential does not change noticeably at the transition.

Above the phase transition, the spectrum is quite different from that in the Coulomb phase. The correlation functions of vector operators (2.2) and (2.3) decay exponentially with approximately the same rate. Therefore either they are both dominated by the same vector state or by two separate vector states with similar masses. The perturbative analysis of the spectrum in the Higgs region in the unitary

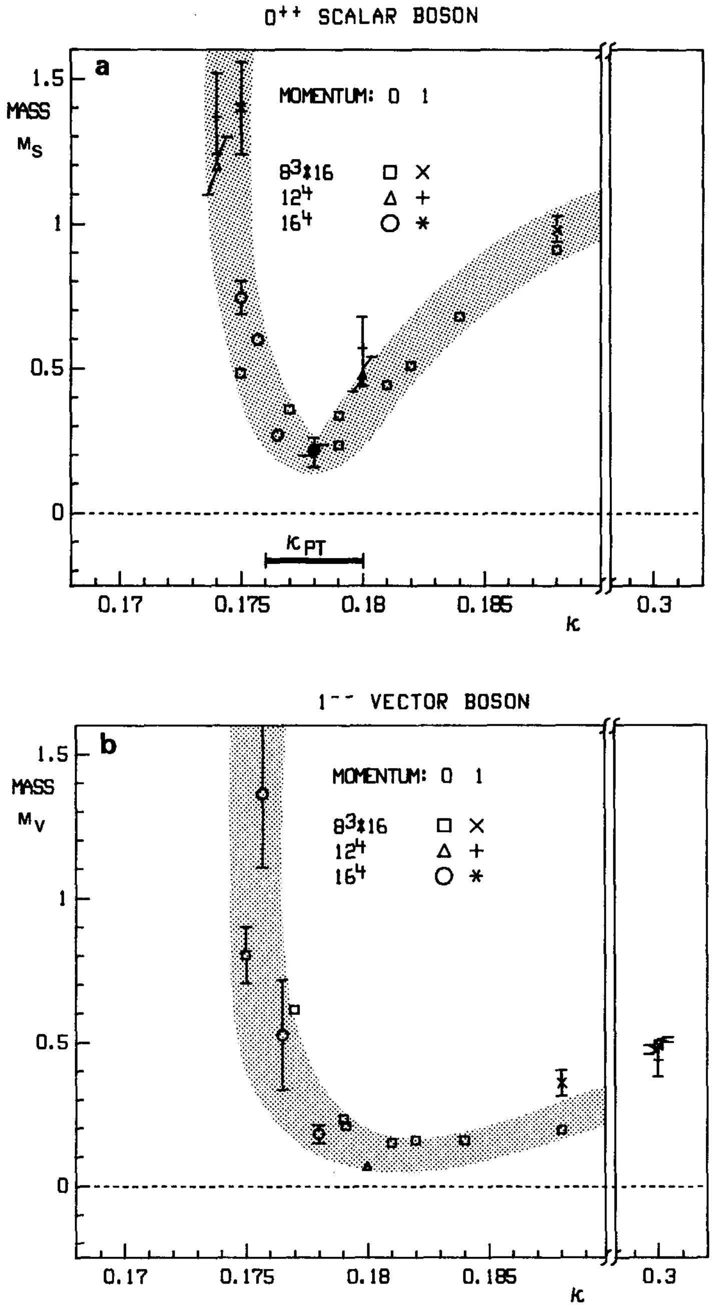


Fig. 2. Masses in lattice units obtained from fits to correlation functions of operators (a) $O_1$, (b) $O_2$, and (c) $O_3$, for three different lattice sizes and for momenta $p = 0$ and $p = 1$, eq. (2.4). The shaded areas represent our estimates of combined statistical and systematical errors. The $\kappa$-scales are discontinuous, emphasizing the Higgs PT region. Technical details are explained in subsect. 2.2.4.

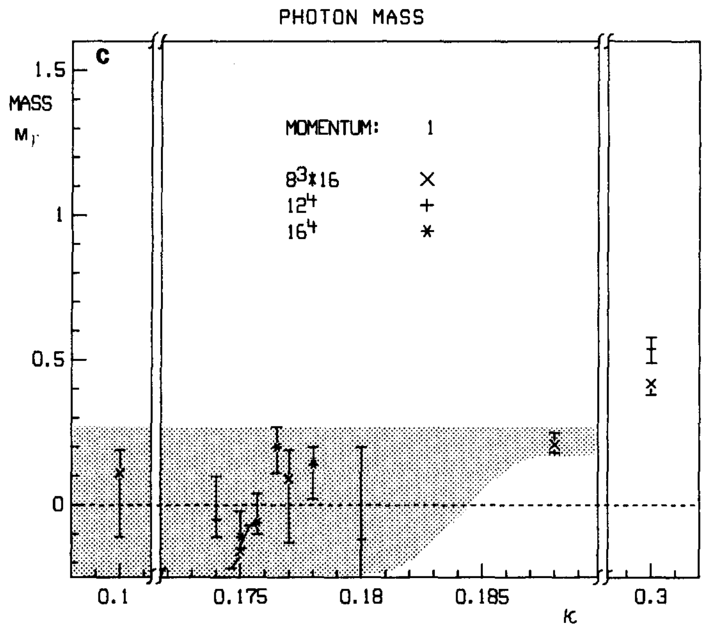


Fig. 2 (continued).

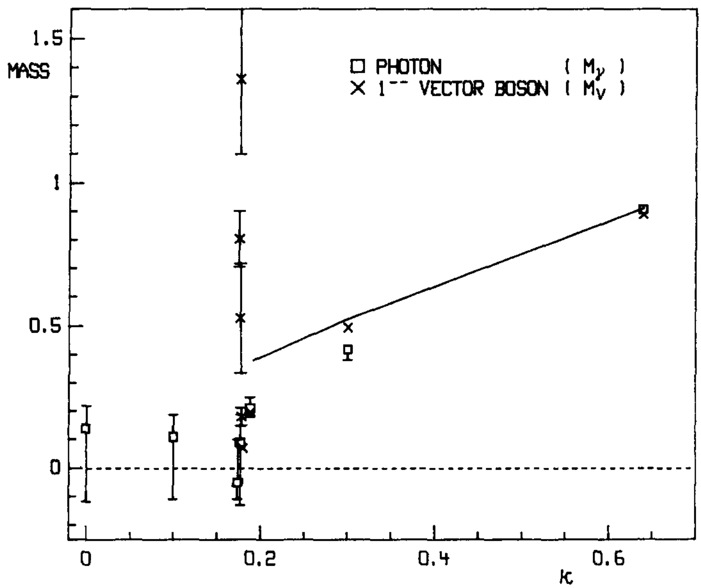


Fig. 3. Representative values of $m_\gamma$ and $m_V$ on a continuous κ-scale covering the whole κ-region that we have investigated. In the Coulomb phase the photon is massless and $m_V$ is very large. In the Higgs region the masses obtained from both correlation functions are indistinguishable. The solid line represents the quasiclassical estimate (2.9) for $m_\gamma$, based on the measured values of $\langle \Phi^* \Phi \rangle$.

gauge suggests that there is only one vector boson present – the massive photon. If this is the case, then the vector bosonium found in the Coulomb phase has no counterpart in the Higgs region. With growing $\kappa$ the massive vector bosonium and the massless photon in the Coulomb phase merge at the Higgs PT to form the massive photon in the Higgs region. We adopt this interpretation of our data for the rest of this paper. The other possibility should not be completely dismissed, however, since some genuinely nonperturbative effects could cause a richer spectrum.

The mass of the photon rises very slowly above the PT and acquires values $m_\gamma \approx 0.5$ at $\kappa = 0.3$ and $m_\gamma \approx 0.9$ at $\kappa = 0.64$. This is consistent with the values of $m_\gamma$ as determined from fits to a lattice Yukawa potential, calculated from the Wilson loops obtained in the same Monte Carlo runs [13]. Therefore the photon becomes massive in the Higgs phase for $\kappa \gg \kappa_{\rm PT}$ in agreement with the standard picture of the Higgs mechanism. In the quasiclassical perturbative approach to the Higgs model one finds

$$m_\gamma^2 \approx 2g^2\kappa\langle\Phi^*\Phi\rangle, \tag{2.9}$$

where $g$ denotes the bare gauge coupling. In fig. 3 we show for comparison the values of $(2g^2\kappa\langle\Phi^*\Phi\rangle)^{1/2}$ in the Higgs region for $\beta = g^{-2} = 2.5$. The quasiclassical estimate is in agreement with the photon mass. (We would like to remark that in ref. [24] one value for $m_{\rm H}/m_\gamma$ has also been obtained by means of duality arguments.)

The Higgs boson mass has a minimum at $\kappa = 0.178(2)$. This position is in full agreement with the location of the transition point as determined from the behaviour of the energy $\mu$ of a screened external charge, an observable most sensitive to the Higgs PT in the U(1) Higgs model [13]. Above the transition the Higgs mass increases much faster than the photon mass and becomes too large to be measured at $\kappa = 0.3$.

*2.2.3. Mass plots.* As we have stressed above, the physical interpretation of states with the same quantum numbers is different in both phases. Nevertheless it is convenient to plot the masses of the states contributing to the same correlation functions in the same figure. Thus we shall use the following notation for both phases:

– scalar boson mass $m_{\rm S}$ (scalar bosonium in the Coulomb phase and Higgs boson in the Higgs region), operator $O_1$,

– vector boson mass $m_{\rm V}$ (vector bosonium in the Coulomb phase and presumably the massive photon in the Higgs region), operator $O_2$, and

– photon mass $m_\gamma$, determined from the $p = 1$ correlation function of operator $O_3$.

These three masses are shown in figs. 2a–c, respectively, as functions of $\kappa$ for several lattice sizes and momenta $p$. In fig. 3 we show representative values of both

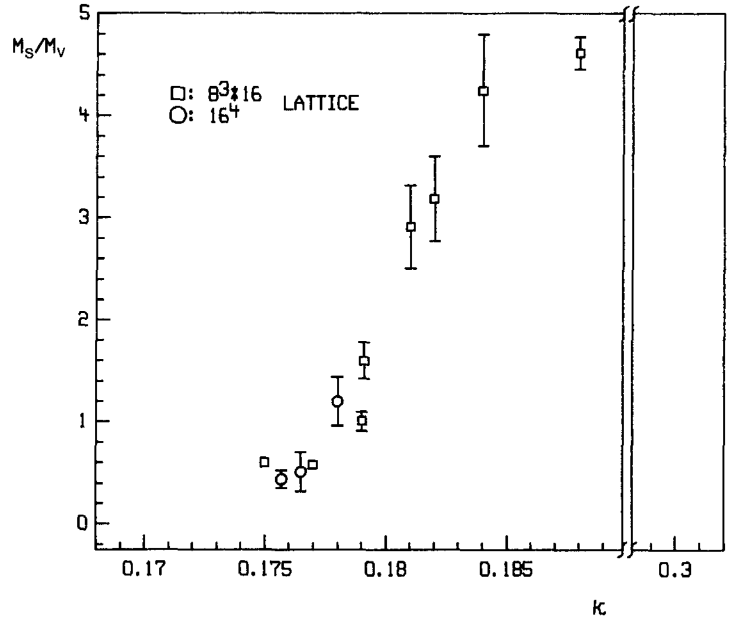


Fig. 4. Ratio $m_S/m_V$ of the scalar and the vector boson masses.

$m_\gamma$ and $m_V$ on a continuous $\kappa$-scale covering the whole $\kappa$-region that we have investigated.

As for figs. 2a and b, the results obtained for the U(1) Higgs model resemble very much those obtained for the nonabelien SU(2) gauge-Higgs model [12]. The mass $m_S$ of the scalar state, which is the Higgs boson mass in the Higgs regions of both models, shows a dip in the vicinity of the Higgs PT. In fig. 4 we show the ratio $m_S/m_V$, which is independent of the lattice spacing. Its $\kappa$-dependence is analogous to that of the ratio of the Higgs and vector boson masses in the SU(2) model. These similarities between both models suggest that also in the SU(2) case the scalar and vector boson states below the Higgs PT [12,25] can be interpreted physically as bound states of SU(2)-doublet constituent scalars. These bound states are analogous to the bosonium in the Coulomb phase of the U(1) model. The confined scalar doublet corresponds to the unconfined charged particle of the U(1) model.

*2.2.4. Comments on the correlation functions.* As mentioned above, all operators have been calculated at momentum $p=0$ and $p=1$. We use the lattice energy-momentum dispersion relation

$$m^2 + 2\sum_{\mu=1}^{3}\left(1-\cos k_\mu\right) = 2(\cosh E - 1)\,. \qquad (2.10)$$

For the correlation functions of the operators $O_1$ and $O_2$, the masses obtained for $p=0$ and $p=1$ are consistent. However, for $p=1$ the errors are substantially larger and we have included only a few of the data for $p=1$ in our figures. When the values of $m^2$ determined through eq. (2.10) were negative, we have plotted $-|m^2|^{1/2}$ instead of $m$ in fig. 2c.

We have also looked at operators with quantum numbers different from the ones presented here, namely $2^{++}$, $1^{+-}$ ($O_3$ with $p=0$), and $0^{+-}$. The correlations of all these operators decay very rapidly and no signal could be extracted. The operator $\Phi^*\Phi$, carrying quantum numbers $0^{++}$, was also considered. It shows a behaviour quite similar to $O_1$ but its signal to noise ratio was worse. The $0^{++}$ plaquette correlation functions gave no measurable signal. We would also like to remark that the fluctuations of the correlation functions are lower in the Higgs region than in the Coulomb phase.

Fig. 2 contains our data on all lattice sizes that we have used. The obtained mass values show no significant dependence on the lattice size. This may be a sign that the correlation length in the scalar channel, which is responsible for the Higgs PT, does not exceed the lattice extension at the Higgs PT for our values of couplings, and is therefore finite [13].

## 3. Other results

### 3.1. SPECIFIC HEAT

In the course of our earlier [9] and the present investigations we obtained results on symmetric lattices of size $L^4$ for $L=4$, 6, 8, 12 and 16 and on asymmetric lattices of size $6^3\times 12$ and $8^3\times 16$. Here we collect the results for the unnormalized specific heat

$$\partial_\kappa\langle\Phi^*U\Phi\rangle = 4L^4\left(\langle[\Phi^*U\Phi]^2\rangle - \langle\Phi^*U\Phi\rangle^2\right) \tag{3.1}$$

on the symmetric lattices. (The normalized specific heat has not been computed in ref. [9].) The peak positions obtained from a fit to these data agree with the determination of $\kappa_{PT}$ from other quantities like e.g. the masses. We obtain the following values:

| $L$ | $\kappa_{PT}$ |
|---|---|
| 4 | 0.1938(6) |
| 6 | 0.1848(1) |
| 8 | 0.1814(1) |
| 12 | 0.17854(1) |
| 16 | 0.177(2) |

(The value of $\kappa_{PT}$ on the $16^4$ lattice has been determined from the position of the discontinuity in the decay parameter $\mu$ of the gauge invariant 2-point function, eq. (2.7), studied in ref. [13].)

Although some of our results indicate that the PT is of weak first order [13] we tentatively apply the finite size scaling relation

$$|\kappa_{PT,L} - \kappa_{PT,\infty}| \approx cL^{-1/\nu}. \tag{3.2}$$

Assuming the $\nu$-value for a free boson theory, $\nu = 0.5$, we get $\kappa_{PT,\infty} = 0.1775(5)$. Without such a restriction on $\nu$ the best fit gives $\kappa_{PT,\infty} = 0.175(1)$ and a value of $\nu = 0.63(1)$. It appears that the dependence of $\kappa_{PT,L}$ on the lattice size is quite similar to that of the $\Phi^4$ theory, although the PT may well be of weak first order.

The height of the specific heat peak does not increase noticeably with growing lattice size, it seems to remain stable from size $8^4$ onwards to larger size, whereas the width definitely continues to decrease. Since the specific heat is the unnormalized one, this phenomenon allows no conclusion about the order of the phase transition.

On the asymmetric lattices the peak of the unnormalized specific heat becomes unexpectedly broader and its height smaller when one changes the lattice from $8^4$ to $8^3 \cdot 16$. A possible interpretation of this phenomenon, which has been observed in spin models as well [26], is based on the notion that the system tries to interpolate between the symmetric $8^4$ and $16^4$ lattices. This would account for the increase of the width of the peak which becomes of the order of $(\kappa_{PT,8} - \kappa_{PT,16})$, whereas the decrease in height would come from the folding of the two sharper peaks. A similar phenomenon has also been observed on a $6^3 \cdot 12$ lattice.

### 3.2. PROBLEMS WITH DIRAC SHEETS

In [9] we reported convergence difficulties in MC runs which occurred when we started with a hot initial configuration in the Coulomb phase. They were caused by long living metastable states. The effect can most clearly be noticed in the plaquette observable, but it is easily seen in the expectation value of $\Phi^*\Phi$, too. It also influences the values of nonlocal observables like the specific heat and masses. Fig. 5 shows a thermal cycle in the expectation value of the plaquette operator, started from a random configuration at $\kappa = 0.06$ in the Coulomb phase. In the thermal cycle one detects a systematic gap between the starting values (lower values of $\langle u_p \rangle$) and the last values in the run causing a fake hysteresis in addition to the effects of the Higgs PT. The upper branch in fig. 5 corresponds to the ground state and thus the initial configuration belongs to an excited state.

To identify the cause of this gap, we have started some thermal runs already at $\kappa = 0$ and we found that the gap extends to the pure U(1) gauge theory. Here the effect has been investigated in detail [16]. It has been found to be caused by the occurrence of a Dirac sheet which is closed due to the periodicity of the lattice

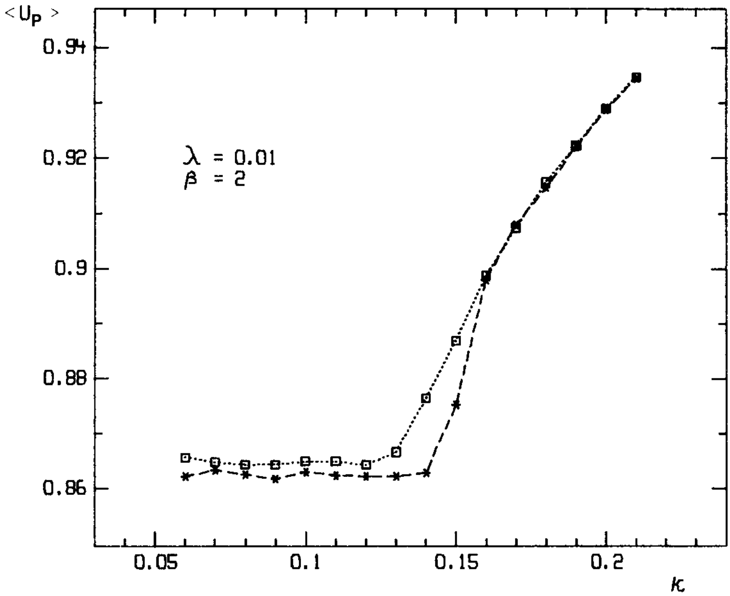


Fig. 5. Expectation values of the plaquette operator $U_P$ in a thermal run performed at $\lambda = 0.01$, $\beta = 2$, as explained in the text. The increased energy in the lower branch is caused by a Dirac sheet.

("trapped magnetic flux"). It can be seen as a remnant of a pair of closed monopole loops winding around the lattice [16]. On a finite lattice there is a significant surplus of energy in plaquettes of one orientation, caused by the magnetic flux. A similar surplus has also been found for finite $\kappa$. Thus we conclude that the gap in the Coulomb phase in fig. 5 is due to the presence of a Dirac sheet, which accidentally vanished during the Higgs PT.

The long lifetime of the excited state corresponding to the lower branch of the fake hysteresis is remarkable. As the energy of a configuration containing the Dirac sheet is higher than that of the ground state, the system is hotter and less ordered. Therefore the Higgs phase transition shifts towards higher values of $\kappa$. We have also observed substantial changes of the specific heat and masses close to the Higgs PT in the configurations with the Dirac sheets.

Although it is easy to avoid the problem with the Dirac sheets by starting with a cold initial configuration of the gauge fields, one has to keep in mind that such a topological effect might disturb one's results.

## 4. Conclusions

We have investigated numerically the spectrum of the compact scalar QED in the vicinity of the Higgs phase transition for large values of the coupling constants, in a region where no reliable analytic methods are available. In the Coulomb phase we have found the massless photon only in the correlation function of the plaquette operator $\mathrm{Im}\, U_{\mathrm{p}}$ at nonzero momentum. The photon does not contribute noticeably to the correlation function of the link operator $\mathrm{Im}\, \Phi^* U \Phi$ with quantum numbers $J^{PC} = 1^{--}$. The latter correlation function reveals the presence of a massive vector state in the Coulomb phase. The state dominating the scalar correlation function is also massive. We have argued that these two heavy states are bosonium states, i.e. bound states of a pair of unconfined bosonic charged particles present in the Coulomb phase. Their masses grow quickly with decreasing $\kappa$, similarly as the mass of the charged particle [13].

Above the Higgs PT, in the Higgs region of the confinement-Higgs phase, the situation is very much like that for the nonabelian SU(2) gauge-Higgs system [12, 25]. We have found the scalar Higgs boson, the mass of which quickly rises with $\kappa$. Both vector correlation functions are dominated either by one and the same state, the massive photon, or possibly by a pair of approximately degenerate vector states. The corresponding mass grows much slower with $\kappa$ than the Higgs boson mass.

In summary, we have found that lattice QED with fundamental scalar charged particles shows a rich spectrum of bound states. In the Higgs region it is in qualitative agreement with the naive expectation from perturbation theory, in the Coulomb phase it follows the conceptions based on the experience from QED.

We are grateful to Prof. H.A. Kastrup for thorough discussions and support and to V. Grösch for help during the computations. We also thank E. Seiler and R.E. Shrock for discussions on the photon mass in the Coulomb phase. The calculations have been performed on supercomputers Cyber-205 at University of Bochum, University of Karlsruhe and SCRI of Florida State University in Tallahassee. The support of these universities and also the assistance of the Rechenzentrum of RWTH Aachen are gratefully acknowledged.

## References

[1] E. Fradkin and S. Shenker, Phys. Rev. D19 (1979) 3682

[2] E. Seiler, Gauge theories as a problem of constructive quantum field theory and statistical mechanics, Lecture Notes in Physics, vol. 159 (Springer 1982)

[3] M. Creutz, L. Jacobs and C. Rebbi, Phys. Reports 95 (1983) 201

[4] M. Creutz, Phys. Rev. D21 (1980) 1006;
K.C. Bowler, G.S. Pawley, B.J. Pendleton, D.J. Wallace and G.W. Thomas, Phys. Lett. 104B (1981) 481;
D.J. Callaway and L.J. Carson, Phys. Rev. D25 (1982) 531

[5] J. Jersák, Review talk given at the Conference Lattice gauge theory—a challenge in large-scale computing, Wuppertal, November 1985, ed. B. Bunk, K.H. Mütter and K. Schilling (Plenum, 1986).

[6] T. Munehisa and Y. Munehisa, Phys. Lett. 116B (1982) 353

[7] H. Kühnelt, C.B. Lang and G. Vones, Nucl. Phys. B230 [FS10] (1984) 16

[8] G. Koutsoumbas, Phys. Lett. 140B (1984) 379;
Y. Munehisa, Phys. Rev. D30 (1984) 1310;

D. Espriu and J.F. Wheater, Nucl. Phys. B258 (1985) 101;
V.P. Gerdt, A.S. Ilchev and V.K. Mitrjushkin, Yad. Fiz. 43 (1986) 736
[9] K. Jansen, J. Jersák, C.B. Lang, T. Neuhaus and G. Vones, Phys. Lett. 155B (1985) 268; Nucl. Phys. B265 [FS15] (1986) 129
[10] R.E. Shrock, Phys. Lett. 162B (1985) 165; 180B (1986) 269; Nucl. Phys. B267 (1986) 301;
I-H. Lee and J. Shigemitsu, Phys. Lett. 169B (1986) 392; Nucl. Phys. B276 (1986) 580
[11] J. Jersák, C.B. Lang, T. Neuhaus and G. Vones, Phys. Rev. D32 (1985) 2761;
H.G. Evertz, V. Grösch, J. Jersák, H.A. Kastrup, D.P. Landau, T. Neuhaus and J.-L. Xu, Phys. Lett. 175B (1986) 335
[12] H.G. Evertz, J. Jersák, C.B. Lang and T. Neuhaus, Phys. Lett. 171B (1986) 271
[13] H.G. Evertz, V. Grösch, K. Jansen, J. Jersák, H.A. Kastrup and T. Neuhaus, Nucl. Phys. B285 [FS19] (1987) 559
[14] K. Fredenhagen and M. Marcu, Commun. Math. Phys. 92 (1983) 81; Phys. Rev. Lett. 56 (1986) 223
[15] K. Osterwalder and E. Seiler, Ann. Phys. 110 (1978) 440
[16] V. Grösch, K. Jansen, J. Jersák, C.B. Lang, T. Neuhaus and C. Rebbi, Phys. Lett. 162B (1985) 171
[17] R.C. Johnson, Phys. Lett. 114B (1982) 147;
B. Berg and A. Billoire, Nucl. Phys. B221 (1983) 109
[18] B. Berg and C. Panagiotakopoulos, Phys. Rev. Lett. 52 (1984) 94
[19] J. Fröhlich and T. Spencer, Commun. Math. Phys. 83 (1982) 411
[20] J. Jersák, T. Neuhaus and P.M. Zerwas, Nucl. Phys. B251 [FS13] (1985) 299
[21] D. Brydges, J. Fröhlich and E. Seiler, Nucl. Phys. B152 (1979) 521;
D.C. Brydges and E. Seiler, J. Stat. Phys. 42 (1986) 405;
C. Borgs and F. Nill, Phys. Lett. 171B (1986) 289
[22] I-H. Lee and J. Shigemitsu, Nucl. Phys. B263 (1986) 280
[23] A. Hasenfratz, P. Hasenfratz, Z. Kunszt and C.B. Lang, Phys. Lett. 110B (1982) 289
[24] H. Kleinert, Phys. Rev. Lett. 56 (1986) 1441
[25] I. Montvay, Phys. Lett. 150B (1985) 441; Nucl. Phys. B269 (1986) 170;
W. Langguth and I. Montvay, Phys. Lett. 165B (1985) 135;
W. Langguth, I. Montvay and P. Weisz, Nucl. Phys. B277 (1986) 11
[26] T. Graim and D.P. Landau, Phys. Rev. B24 (1981) 5156